Review article **Open Access**

Abhinav Parihar, Nikhil Shukla, Matthew Jerry, Suman Datta and Arijit Raychowdhury*

Computing with dynamical systems based on insulator-metal-transition oscillators

DOI 10.1515/nanoph-2016-0144
Received August 14, 2016; revised November 10, 2016; accepted December 4, 2016

Abstract: In this paper, we review recent work on novel computing paradigms using coupled oscillatory dynamical systems. We explore systems of relaxation oscillators based on linear state transitioning devices, which switch between two discrete states with hysteresis. By harnessing the dynamics of complex, connected systems, we embrace the philosophy of "let physics do the computing" and demonstrate how complex phase and frequency dynamics of such systems can be controlled, programmed, and observed to solve computationally hard problems. Although our discussion in this paper is limited to insulator-to-metallic state transition devices, the general philosophy of such computing paradigms can be translated to other mediums including optical systems. We present the necessary mathematical treatments necessary to understand the time evolution of these systems and demonstrate through recent experimental results the potential of such computational primitives.

Keywords: coupled oscillators; phase transition; image analytics.

1 Introduction

Computing is the backbone of the modern society; from economics to security and scientific advancement to social welfare, each and every aspect of our lives has been enriched by the technology revolution. We have enjoyed the benefits of Moore's Law over the last four decades as technology scaling brought the power of supercomputers to our Smartphones. With increasing challenges in scaling came ground-breaking innovations in the transistor technology. As we look ahead, limits of traditional scaling are already in sight. The demise of Dennard scaling and slowing down of Moore's Law have further exposed the fundamental scaling limitations of the Von Neumann execution models of computing. This transition is accompanied by the realization that in a fast-evolving, socially interconnected world, we are observing a seismic shift in the amount of unstructured data that need to be processed in real-time, and consequently, future systems will be limited by the energy growth of data movement rather than that of compute. Therefore, we need fundamentally new approaches to sustain the exponential growth in performance beyond the end of the Complementary metal–oxide–semiconductor (CMOS) roadmap. This will require new execution models, coupled with new devices to implement them. In particular, we observe that new models that deal with data analytics have compute and storage interleaved in a fine-grained manner – not separated as in the Von Neumann world. Moving forward, computing technology will heavily penalize separation of data and compute and we need to marry them in better ways to handle emergent applications. This may necessitate that barriers of abstraction are broken. Next generation of computational models should map natively to the physics and dynamics of the physical devices, without a Boolean abstraction. Of course, it is a fool's endeavor to assume that the Von Neumann architecture will perish; rather, newer computing models and dedicated hardware accelerators will supplement traditional Von Neumann machines in "data- centric" tasks.

In today's computing landscape, ever harder problems are being encountered each day. From social networks to graph analytics, from weather prediction to scientific computation, computationally hard problems are present everywhere. Some of these problems are challenging just because of the sheer size of the datasets, but many other problems like optimization problems, although small in size, are intractable because of their inherent complexity and often combinatorial nature of solution spaces [1]. The sequential Von Neumann machine has been useful for

***Corresponding author: Arijit Raychowdhury,** Georgia Institute of technology, School of Electrical and Computer Engineering, Atlanta, GA 30332, USA, e-mail: arijit.raychowdhury@ece.gatech.edu
Abhinav Parihar: Georgia Institute of technology, School of Electrical and Computer Engineering, Atlanta, GA 30332, USA
Nikhil Shukla, Matthew Jerry and Suman Datta: University of Norte Dame, Department of Electrical Engineering, Notre Dame, IN 46556, USA

most problems we have encountered in the past, but as the complexity of problems increases, significant research is underway for alternative paradigms, architectures, and hardware that can be used for solving complex problems more efficiently. Most of these efforts borrow essential ideas from natural computing processes. These include distributed computing, distributed memory, integrated processing and memory, shifting information representation from symbolic to physically meaningful quantities, and switching from sequential discrete time to continuous time dynamics.

Among the different problems of interest, associative computing, scientific computing [including solution of coupled partial differential equations (PDEs)], and optimizations form important classes of data-centric as well as model-centric computations. Active research in all these areas suggests that analog or continuous time systems may offer alternative faster and more energy-efficient solutions that their traditional digital counterparts. For example, in case of hard optimization problems, alternative paradigms and architectures include, but are not limited to, cellular automata [2], quantum computing [3], Ising model based systems [4, 5], neural networks [6], stochastic searching architectures [7], and memcomputing [8]. Among architectures for solving PDEs, cellular neural networks (CNNs) have been studied [9, 10]. Some studies have also suggested using cellular automata for solving PDEs [11].

The basic philosophy of most of these networks for optimization, e.g. artificial neural networks, is to first come up with an energy function that can be a penalty function or a rewarding function depending on how far the current solution is from the optimal solution [6]. The next step is to tune the parameters of the network such that as time evolves, the dynamics of the system decreases the penalty function or increases the reward. But even if such a massively parallel system is devised, which can solve NP-hard optimization problems, exponential resources of space, time, or precision will be required [12, 13]. Another direction is often explored where instead of trying to solve the optimization exactly, an approximation is targeted, which works well for most problems on average and allows less optimal solutions in harder instances. There can be other kinds of trade-offs like in the case of Hopfield networks where even though the optimal solution maps exactly to global minima, there can be too many local minima where the system can get trapped. Finally, the physical layer of computing, namely the semiconductor device platform, needs to be able to support such systems and the CMOS transistor is not always an optimal device choice.

Recently, the development of novel phase transition materials like vanadium dioxide (VO_2) and corresponding electronic devices, which show insulator-to-metal transitions (IMTs) [14], has sparked interest in creating compact relaxation oscillators [15, 16]. These oscillators, when coupled to each other, exhibit phase synchronization, which can be used for phase-based computing. Such new kinds of devices present interesting opportunities to create systems with novel synchronization dynamics. The impact of using such devices as basic units in circuits can break the abstraction between the physical and the algorithmic layers of computing. It should be noted that the synchronization dynamics of coupled oscillators not only have a wide variety of applications in engineering but also explain many natural, chemical, and biological synchronization phenomena like the synchronized flashing of fireflies, pacemaker cells in the human heart, chemical oscillations, neural oscillations, and laser arrays, to name a few. These novel computing primitives, of course, are neither drop-in replacements for CMOS transistors nor straightforward extensions of the existing computing architectures. It requires rethinking of the basic computational entities in new kinds of system architectures. In this paper, we review some computational models using coupled relaxation oscillators based on VO_2 metal-insulator transition (MIT) devices focusing on how the system dynamics can be modeled and the applications they can enable. We limit our discussion on applications in image processing for the sake of brevity. However, the potential of dynamical systems extends far beyond image analytics and promises to be a competing computational model for post-CMOS technologies.

2 A perspective on coupled oscillatory networks

The area of coupled oscillators has been dominated mostly by theoretical models and numerical simulations but has very few successful physical implementations. The reason is that the assumptions made for analytical simplification in those theoretical models are too difficult to realize in practice. Also an important limitation of such systems, which is true for any dynamical system, is that if a dynamical system is able to solve computationally hard (NP-class) problems exactly, then it necessarily has to be chaotic in nature, which would require exponential precision in both simulations and physical implementations.

The most popular coupled oscillator models in this area are the Kuramoto oscillator models [17], which rely

on sinusoidal oscillators coupled using "weak" and linear phase coupling. A Kuramoto system of N oscillators is described by the following:

$$\dot{\theta}_i = \dot{\omega}_i + \frac{K}{N}\sum_{j=1}^{N}\sin(\theta_j - \theta_i),\ i = 1,\ \ldots,\ N,$$

where θ_i and ω_i are the phase and frequency, respectively, of ith oscillator. Major challenges in this kind of coupled oscillator model are the notion of weak coupling, i.e. $K \ll N$, and the idea that the coupling effects phase only without disturbing the frequencies. Moreover, creating arrays of compact sinusoidal oscillators with many oscillators coupled to each other poses serious challenges given the requirements. Similar models of weak linear phase coupling were also explored for Van Der Pol oscillators [18], which have an additional nonlinearity. But the implementation of such oscillators is also non-trivial, and the coupling behavior becomes too complicated to tackle large, connected networks [19–22].

Nevertheless, the ability of coupled oscillatory systems to encode computing has long been realized. Associative computing, with applications in pattern detection and machine learning, has been demonstrated in theory. Similarly oscillatory CNNs have been shown to possess extraordinary computing ability in solving problems as varied as template matching, PDEs and ODEs, and so on. More recently, this effort has been augmented by advances in the development of compact oscillators in non-silicon technologies. One prominent effort is the use of spin torque oscillators (STOs) coupled with using spin diffusion currents and providing a computational platform for machine learning, spiking neural networks, and others [23, 24]. However, the high current densities of STOs and the limited range of spin diffusion currents continue to pose serious challenges to technologists.

In our studies, we explore phase transition based relaxation oscillators with piecewise linear dynamics, which means the system is described by different linear dynamical systems in different "states" of the system. These states are basically charging and discharging of a capacitive element. The coupling is also electronic and is accomplished by linear capacitors and/or resistors. The repeated switching between these states gives rise to oscillatory behavior and the notion of phase. But because the switching is itself determined by the state variables (voltage thresholds) and not explicitly by time, the coupling dynamics and hence the overall system dynamics are often mathematically intractable and closed-form approximations like the Kumamoto model are not possible. This further complicates the analysis when the goal is to perform computation in phase space. Hence, model development coupled with numerical analysis and an intuitive understanding of how complex systems evolve over time become essential tools to engineer such systems. The relaxation oscillators we investigated are built using phase change devices, which are devices that switch states between a metallic state with low resistance and insulating state with high resistance depending on the voltage across them. In the next section, we will describe simple mathematical constructs that can assist in analyzing these oscillators and the results obtained once they are coupled electrically.

3 Relaxation oscillators based on phase change devices

3.1 State-changing devices

The state-changing devices we consider are essentially linear conductances (or resistances) but can transition between two conducting states – insulating state with conductance g_{di} and metallic state with conductance g_{dm}. We assume that $g_{dm} \gg g_{di}$. They are also called IMT devices. We use VO_2 as the material choice. A state transition is triggered by the voltage applied across the devices as well as the history. When the voltage across the device increases above a higher threshold voltage V_h, the device changes its state to metallic with conductance g_{dm}, and when the voltage decreases below a lower threshold V_l, it changes to insulating state with conductance g_{dl}. There is hysteresis in switching, i.e. $V_h \neq V_l$, which means when the voltage applied is between V_h and V_l, the device retains the last state it was in. An internal capacitance is associated with the device that ensures gradual buildup and decaying of the voltage (and energy) across the device. Rigorous mathematical analysis of such oscillator configurations can be found in Ref. [25].

3.2 Single oscillator configurations

There can be multiple configurations/circuits of a relaxation oscillator based on state-changing device. On a simplistic level, two basic configurations exist – (a) two state-changing devices in series, called D-D, where D stands for device (Figure 1A), and (b) a state-changing device in series with a resistance, called D-R (Figure 1B). In the former, the charging and discharging rates are

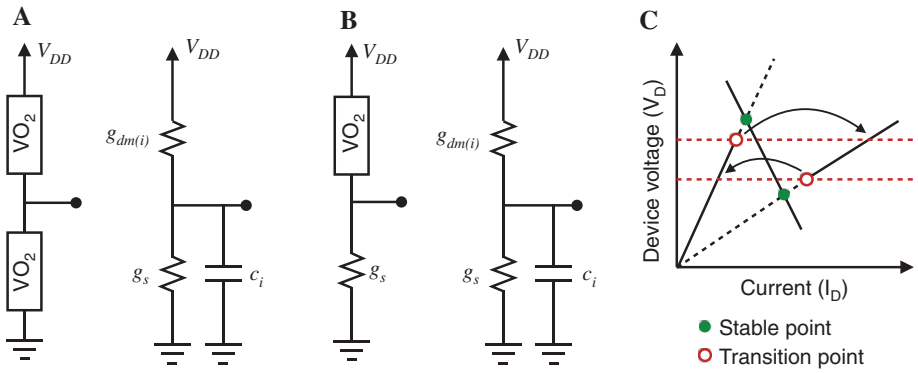

Figure 1: (A) D-D oscillator circuit configuration and its equivalent circuit. (B) D-R oscillator circuit configuration and its equivalent circuit. (C) Load line graph for the D-R circuit and the region of operation of D-R oscillator. When the stable points (green filled points) are outside the region of operation, the system shows oscillations.

equal, but they are different in the latter. The functioning of the two circuits is as follows.

In case of two devices in series D-D, the two devices must be in opposite conduction states (one metallic and the other insulating) all the time for oscillations to occur. If the threshold voltages v_l and v_h are equal for the devices and the following condition holds:

$$V_l + V_h = V_{DD} \tag{1}$$

and at $t=0$, the devices are in different conduction states, then any time one device switches, the other will make the opposite transition as well. As $g_{dm} \gg g_{di}$, the devices can be considered as switches, which are open in insulating state and closed in metallic with conductance g_{dm}. The mechanism of oscillations is essentially charging and discharging of the internal capacitances of the devices. The device in metallic state connects the circuit and charges (discharges) the lumped internal capacitance. The voltage at the output node increases (decreases) and eventually reaches the threshold voltage. Because of (1), both devices will switch at the same time, causing their behavior to switch. The charging (discharging) becomes discharging (charging), and the cycle continues. The modeling of a D-D oscillator is as follows. All the lowercase voltages referred in the paper are normalized voltages with respect to V_{DD}, which means $v_h = V_h/V_{DD}$ and $v_l = V_l/V_{DD}$. Also v_{dd} is used as normalized and hence $v_{dd}=1$.

The single D-D oscillator can be described by the following set of piecewise linear differential equations:

$$cv' = \begin{cases} (v_{dd} - v)g_{1dm} & \text{charging} \\ -g_{2dm} & \text{discharging} \end{cases},$$

where g_{1dm} and g_{2dm} are metallic conductances of the two devices, respectively. As $g_{di} \gg g_{dm}$, there is no term involving g_{di} in the equations. The equation can be re-written as follows:

$$cv' = -g(s)v + p(s)$$

where s denotes the conduction state of the device (0 for metallic and 1 for insulating) and $g(s)$ and $p(s)$ depend on the device conduction state s, as follows:

$$g(s) = \begin{cases} g_{1dm}, & s=0 \\ g_{2dm}, & s=1 \end{cases}$$

$$p(s) = \begin{cases} g_{1dm}, & s=0 \\ 0, & s=1 \end{cases}.$$

For D-R oscillators, the oscillations occur due to a lack of stable point as seen in the load line graph of Figure 1C. Solid sloped lines are the regions of operation of the device in insulating and metallic states, respectively. The system does not enter the dashed sloped lines as a transition occurs to the other conduction state at the red points. The stable points, denoted by green points, are the points where the load line intersects the I-V curve of the device. These stable points in each state lie outside the region of operation of the circuit, and hence, the circuit shows self-sustained oscillations. This is a much more practical configuration from an electrical implementation point of view, as the conditions required for oscillations are not very strict. Following a similar analysis as in the D-D oscillator case, the dynamics of the single D-R oscillator can be described as follows:

$$cv' = \begin{cases} (v_{dd} - v)g_{dm} - vg_s & \text{charging} \\ -vg_s & \text{discharging} \end{cases},$$

which can be re-written as follows:

$$cv' = -g(s)v + p(s),$$

where

$$g(s) = \begin{cases} g_{dm} + g_s, & s = 0 \\ g_s, & s = 1 \end{cases}$$

$$p(s) = \begin{cases} g_{dm}, & s = 0 \\ 0, & s = 1 \end{cases}$$

and s denotes the conduction state of the system as before. Detailed analysis of configurations and modeling of such oscillators can be found in Ref. [25].

3.3 Pairwise coupling

Analysis of two coupled relaxation oscillators can give interesting insights into how such coupling dynamics can be used in various computing applications and can also help understand and exploit dynamics from complex couplings. There can be many ways in which the oscillators can be coupled. We have looked at coupled oscillator circuits where the oscillators are coupled through their output nodes using a capacitance, a resistance, or a parallel RC combination (Figure 2).

3.3.1 D-D oscillators

The D-D configuration, although difficult in an electrical implementation point of view, is very simple to analyze and gives interesting insights about dynamics of such piecewise linear systems. Two identical D-D oscillators coupled using a RC circuit can be modeled as follows. When coupled, the system has four conduction states $s = s_1 s_2 \in \{00, 01, 10, 11\}$ corresponding to the four combinations of s_1 and s_2. The coupled system can be described in matrix form as follows:

$$c_c F x'(t) = -g_c A(s) x(t) + P(s)$$

$$x'(t) = -\frac{g_c}{c_c} F^{-1} A(s)(x(t) - A^{-1}(s)P(s)),$$

where $x(t) = (v_1(t),\ c_1(t))$ is the state variable at any time instant t. The 2×2 matrices F and $A(s)$ and vector $P(s)$ are given by the following:

$$F = \begin{bmatrix} 1+\alpha_1 & -1 \\ -1 & 1+\alpha_2 \end{bmatrix}$$

$$A(00) = \begin{bmatrix} -\beta_{11} - 1 & 1 \\ 1 & -\beta_{21} - 1 \end{bmatrix}, \quad P(00) = \begin{bmatrix} \beta_{11} \\ \beta_{21} \end{bmatrix}$$

$$A(10) = \begin{bmatrix} -\beta_{12} - 1 & 1 \\ 1 & -\beta_{21} - 1 \end{bmatrix}, \quad P(10) = \begin{bmatrix} 0 \\ \beta_{21} \end{bmatrix}$$

$$A(01) = \begin{bmatrix} -\beta_{11} - 1 & 1 \\ 1 & -\beta_{22} - 1 \end{bmatrix}, \quad P(01) = \begin{bmatrix} \beta_{11} \\ 0 \end{bmatrix}$$

$$A(11) = \begin{bmatrix} -\beta_{12} - 1 & 1 \\ 1 & -\beta_{22} - 1 \end{bmatrix}, \quad P(11) = 0$$

Here, $\alpha_i = c_i / c_c$ is the ratio of the combined lumped capacitance of ith oscillator to the coupling capacitance c_c, and $\beta_{ij} = g_{ijdm} / g_c$ is the ratio of the metallic state conductance of jth device of ith oscillator to the coupling conductance, where $i \in \{1, 2\}$ and $j \in \{1, 2\}$. The fixed point in a conduction state s is given by $p_s = A^{-1}(s)P(s)$, and the matrix determining the flow (the *flow matrix* or the *velocity matrix*) is given by $\frac{g_c}{c_c} F^{-1} A(s)$.

When two identical D-D oscillators are coupled using a parallel RC circuit with coupling resistance $R_C = 1/g_c$ and coupling capacitance C_C, they can lock in-phase or anti-phase depending on the relative values of R_C and C_C. In the extreme case of purely capacitive coupling with $g_c = 0$, the anti-phase locking orbit is stable and the in-phase locking orbit is unstable. In case of purely resistive coupling with $C_C = 0$, the in-phase locking orbit is stable and the anti-phase locking orbit is unstable. For other values, the system always has in-phase locking periodic orbit as well as anti-phase periodic locking orbits, with the stable locking being the in-phase locking when the coupling is close to purely resistive, and when the coupling is close to purely capacitive, the stable locking is the anti-phase locking. Interestingly, considering the parameter space of R_C and C_C, there exists a region with bistable orbits, i.e. both the in-phase and anti-phase orbits are stable. In this region, the steady-state locking depends on the initial starting voltages at $t = 0$ of the oscillators.

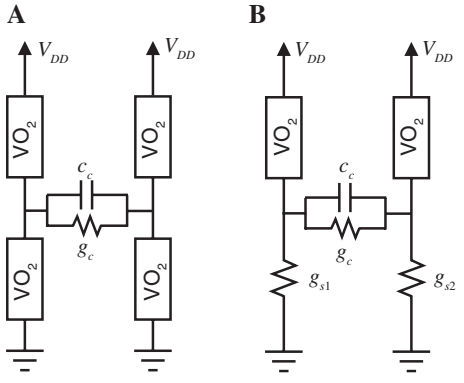

Figure 2: D-D (A) and D-R (B) coupled oscillator circuits using parallel RC circuit as the coupling circuit.

3.3.2 D-R oscillators

From a computing application point of view, pairwise coupled D-R oscillators have interesting applications. When the series resistances are replaced by transistors, as shown in Figure 3, and the coupling is a simple capacitive coupling, a pair of coupled D-R oscillators can be used as an analog comparator whose output has the form of a difference norm [16, 26, 27]. Typical steady-state orbits of the coupled system plotted in a $v_1 \times v_2$ plane are shown in Figure 4A. When $v_{gs1}-v_{gs2}$ increases, the steady-state orbits of the oscillators get deformed. Such deformation of the steady-state orbits can be measured using a simple averaged thresholding-and-XOR operation on the steady-state outputs of the oscillators. This averaged XOR measure is defined as, first, thresholding the output to binary values; second, applying XOR operation on these binary values at every time instant; and finally, averaging this XOR output over some time duration. The averaged XOR output as a function of v_{gs1} and v_{gs2} is shown in Figure 4B. The XOR surface reaches minimum value along the line $v_{gs1}=v_{gs2}$. Within the locking range, it rises as an even function of $v_{gs1}-v_{gs2}$ resembling a difference norm. Outside the locking range, it averages to about 0.5. These characteristics of the curve can be explained by realizing that the averaged XOR measure by construction is equal to the fraction of the time the system spends in the grey region (region where XOR output is 1 – determined by the thresholds on v_1 and v_2) in steady state, as shown in Figure 4A. It can be seen

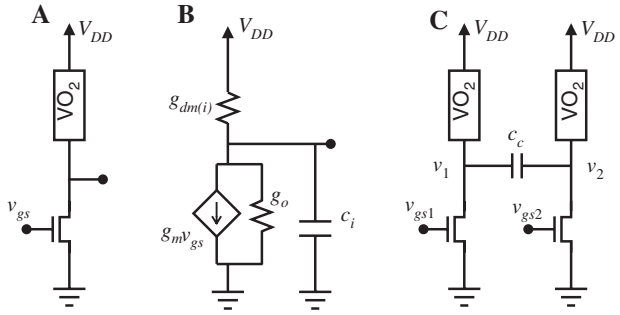

Figure 3: (A) Oscillator circuit with MOSFET in series with a VO_2 device. (B) Small signal equivalent circuit of the oscillator with VO_2 in series with a MOSFET. (C) Coupled oscillator circuit with a series MOSFET in place of a series resistance.

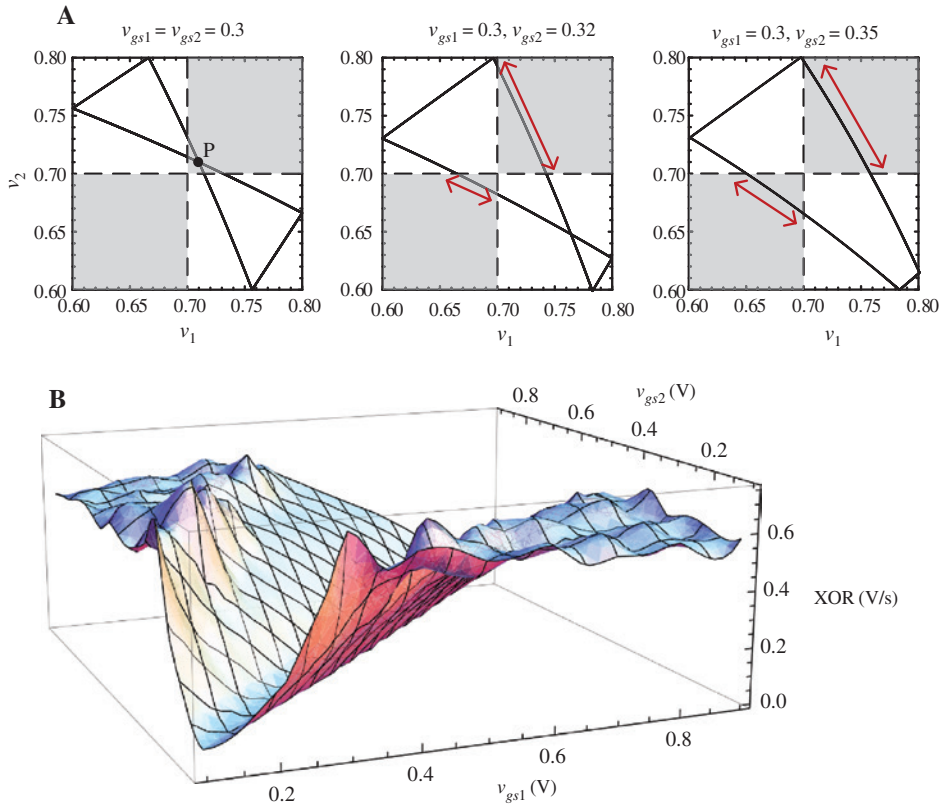

Figure 4: (A) Relationship between XOR output and the steady-state periodic orbit of the system. At any instant of time, XOR output is 1 in the grey region and 0 otherwise. Averaged XOR output is equal to the fraction of time spent by the system in the grey regions. XOR output is minimum in case of a butterfly-shaped orbit (left) and should increase as the orbit transitions to a rectangular orbit (right). (B) XOR surface as a function of v_{gs1} and v_{gs2}.

that the XOR measure should have the lowest value in the symmetric case $v_{gs1} = v_{gs2}$ when the system locks out-of-phase and should increase as values diverge. Such a system can be used as an analog comparator with output as a difference norm. Arrays of such comparators can be used for template matching applications where element-wise comparisons suffice to decide a match.

4 IMT oscillators

4.1 IMT basics

VO_2 undergoes a first-order metal-insulator phase transition marked by an abrupt change in conductivity up to five orders in magnitude. This abrupt change in conductivity, which is also accompanied by changes in optical properties and can be triggered externally using thermal [28], optical [29], electronic [30], or strain [31] stimuli, can pave the way for novel electronic devices including steep slope switching devices, memory elements, and ultra-fast optical switches. One of the characteristic features of the electrically driven first-order MIT in VO_2 is its inherently hysteretic nature, as shown in Figure 5A. In previous publications, we demonstrated an electric field driven non-hysteretic phase transition in VO_2 and showed novel device functionalities like coupled oscillations that may enable efficient implementation of novel, non-Boolean computing models. The electrically driven first-order phase transition results in abrupt switching in conductivity but always comes at the cost of an intrinsic hysteresis, because the electrical field at which IMT occurs is always higher than that at which the MIT happens. Further, the electrically driven phase transition in VO_2 is also accompanied by a dramatic reduction in the optical transmission across the IMT [32]. These optical properties can not only be used as a probe for understanding the fundamental physics of the phase transition but also be harnessed for engineering phase transition devices and circuits, as discussed in Section 4.2. In our experiments, VO_2 is epitaxially grown on (001) TiO2 (−0.86% compressive strain) using molecular beam epitaxy (MBE), then patterned to form channels and followed by deposition of Au/Pd contacts to electrically access the VO_2 channel. First, the device is electrically driven across the phase transition boundary with zero external series resistance. A current compliance is set to limit the current in the metallic state (to prevent excess Joule heating resulting in permanent damage). The IMT and the reverse MIT occur at two critical fields, E_2 and E_1, respectively. The critical field E_2 is the field required to attain the Mott criteria and thereby triggers the formation of the metallic phase. As transport in the insulating phase is dominated by hopping transport, we use the field-dependent hopping conductance to understand its electrical properties.

The negative differential resistance (NDR) region, where VO_2 is characterized by a conductivity intermediate between the metallic and insulating states, is referred to as the phase coexistence region. The net conductivity in this region is due to contributions from the metallic and insulating phase. *In situ* nano XRD characterization performed simultaneously with the transient waveform measurement confirms that the nature of the insulating phase is Monoclinic M1 and that of the metallic phase is Rutile, which is expected as the films are −0.86% compressively strained. When such a phase transition device is operated in the hysteretic region, it breaks into spontaneous oscillations, as shown in Figure 5B. This is a relaxation oscillator with piecewise linear dynamics, as has been discussed in the previous section.

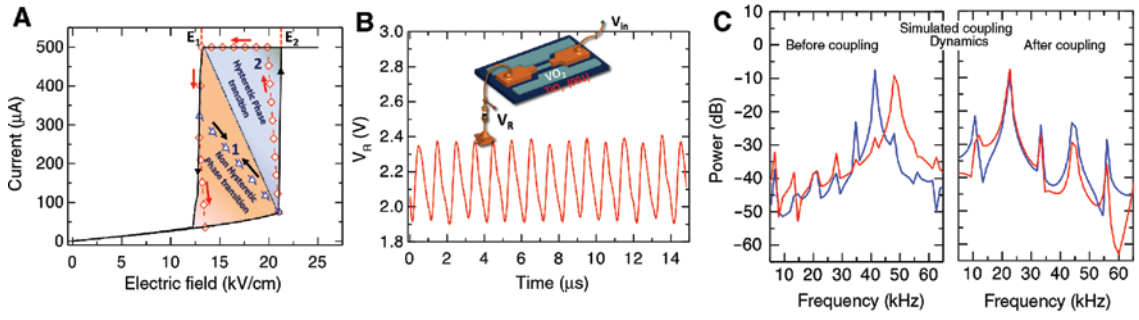

Figure 5: (A) Measured I-E characteristics of a VO_2 device illustrating the hysteretic window. (B) Measured characteristics show oscillations when biased with a pull-down resistor. (C) Measurements and simulations illustrate frequency locking when two oscillators are coupled electrically.

4.2 Coupling IMT oscillators: electrical and optical

While we have focused on electrical devices and coupling schemes using resistors and capacitors as discussed above, our work has significant synergies with nanophotonics and optics. Optical properties of the phase transition materials could be leveraged for designing peripheral circuitry of a chip-scaled coupled oscillator system. For instance, even in the electrical realization (as shown here) of large coupled oscillatory systems, one of the major challenges is to be able to measure simultaneously, speedily, and accurately the phase of the oscillators as the phase dynamics form the fundamental basis of the computational primitive using coupled oscillators. An optical phase read-out scheme can potentially be designed for the oscillators, as the VO_2-based phase transition devices show a significant change in optical response across the phase transition; the optical transmission dramatically reduces as VO_2 undergoes IMT [33]. Further, optically tuned VO_2 has been shown as a memory capacitance and thus can be potentially incorporated as a tunable coupling element in the coupled oscillator system. Additionally, the ability to manipulate the coupling strength using well-known nanophotonics techniques such as colossal electro-optic or thermo-optic effects increases their future potential to realize large-scale on-chip nonlinear dynamical systems.

The ideas and the computational models developed using IMT-based coupled oscillators can also be explored for other oscillatory computing systems. For instance, Ref. [34] demonstrates experimentally the synchronization of a pair of silicon nitride optomechanical oscillators (OMOs) that are optically coupled through the radiation pressure field as opposed to mechanically coupled. The researchers were able to turn the optical coupling on and off using a heating laser via thermos-optic effect.

Overall, this is an area of research that lies unexplored from a computational point of view, and success in creating complex systems with many to many connections will be key to achieving hardware platforms capable of truly delivering the promise of coupled dynamical systems as computational elements.

5 Oscillator networks and applications

5.1 Image data processing and analytics

Arrays of such IMT oscillator based comparators can be used for template matching applications where element-wise comparisons suffice to decide a match. Figure 6A, B illustrates the XOR-ed output of the phases of two coupled oscillators configured as in Figure 3. We observe from Figure 6C, D a close match between experiments and simulations, and it demonstrates that the XOR measure between the outputs of the two oscillators can be used as a measure of distance between two inputs as given by $\Delta V_{GS} = V_{GS1} - V_{GS2}$.

We investigate the application of pairwise coupled oscillators for visual saliency approximations (detecting parts of the image that visually standout). Oscillator-based edge detection is performed using an array of pairwise oscillators to approximate the degree of dissimilarity between a given image pixel and its immediate neighbors. Different edges, vertical, horizontal, diagonal, are detected based on the selection of neighboring pixels for comparison. As this concept is expanded to include the comparison of pixels within a larger neighborhood (pixels surrounding reference pixel; a 3×3 neighborhood is used here), the output approximates the visual saliency. We also note that pairwise coupling of oscillators leads to the inherent calculation of fractional norms between templates and inputs, a task that is notoriously painstaking on a digitally abstracted computer. It is evident from Figure 6E that the coupled oscillators show higher sensitivity to image contrast in comparison to a CMOS ASIC accelerator that uses a linear norm.

We further demonstrate this by comparing images of faces and hand-written numbers, as shown in Figure 6F. We first use the XOR measure for each pixel and calculate the number of pixels with XOR output below a threshold value. Figure 6F shows the results of comparing faces with a relaxation comparator, where the grey shade corresponds to the fraction of pixels with positive match, white being the highest. Such system followed by a winner-take-all (WTA), i.e. a threshold on the number of pixels that give a positive match, can be used to decide if the input image matches a stored template pattern. The value is chosen around 0.2 considering the minimum values of the XOR surface in the operating range of values. The two thresholds described above depend on different factors. The threshold of the number of pixels for WTA would depend on the database and the error statistics required or estimated. On the other hand, it would be decided more by the nature of the XOR surface (Figure 4B) and its minimum values.

A coupled VO_2-MOSFET configuration cascaded with a XOR provides a way of measuring a form of fractional distance using FSK. Such associative networks can be used in more complex pattern matching and classification problems with potentially large benefits in energy efficiency. The advantages of such oscillator

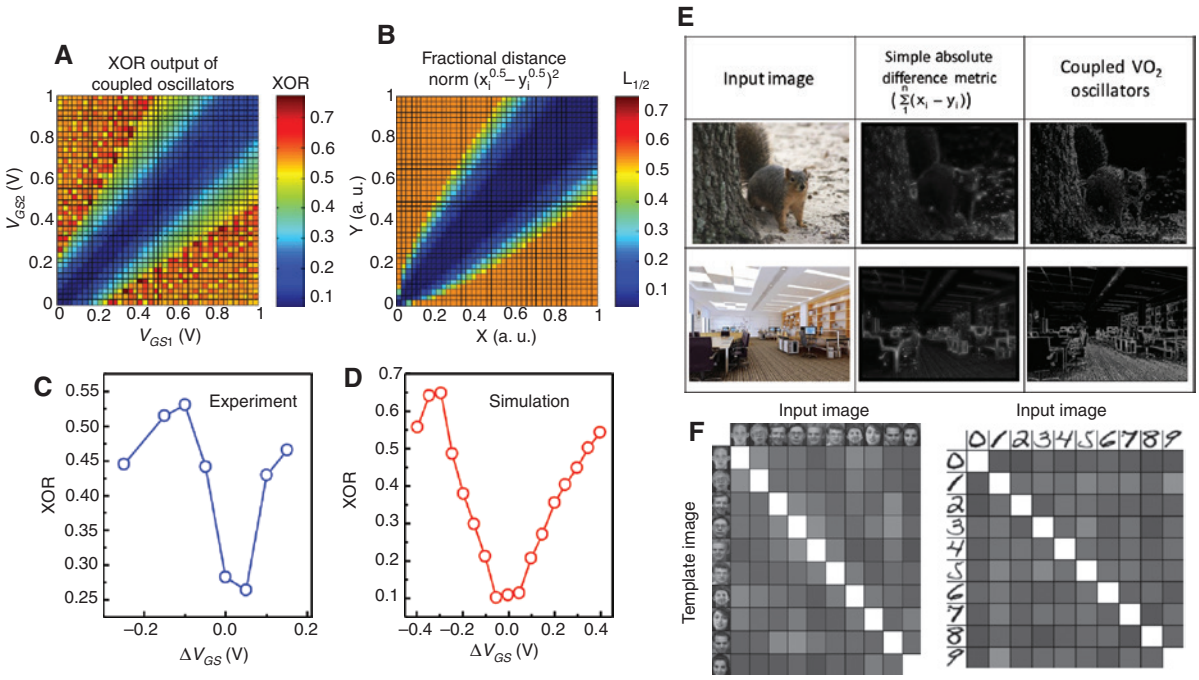

Figure 6: (A, B) XOR output of pairwise coupled oscillators shows close similarity with fractional norm measure between two inputs. (C, D) Experimental results and simulations reveal the capability of coupled oscillator phases to encode a measure of difference between two inputs (ΔV_{GS}). (E) Saliency detection of images using coupled oscillator systems and a digital implementation, (F) a pairwise XOR measure is extended to illustrate pattern matching between an input and a template. A lighter color corresponds to a better match.

based computing systems can be truly harnessed if they are miniaturized, made compact, and integrated. The authors would like to note that the technological realization of such a coupled oscillator system would have to account for variation effects such as device-to-device variations (switching speed, switching voltages and currents, hysteresis) in VO_2 as well as variations in the series transistor such as threshold voltage mismatch among the FETs and their effects on algorithms as well as on computational performance. While a holistic study of variation effects will require the development of systems beyond small prototypes currently under investigation, the authors have addressed some of the effects of variations on computational tasks such as pattern matching in previous publications [27].

We expect such systems to provide large improvements in energy efficiency, opening up possibilities in areas as varied as surveillance, consumer electronics, and in-sensor processing. For comparison, a digital baseline design is designed and simulated. All digital circuits are implemented with 11-nm node transistor models. We observe that the coupled oscillators provide a power reduction of 20× over CMOS, reflecting the advantage of letting physics do the computing approach and potentially removing the Boolean bottleneck. For further details, interested readers are pointed to the previous work by the authors [16].

5.2 Complex global connections and possibilities for computation

The full computational power of such coupled dynamical systems can be further harnessed using complex global interactions among oscillators instead of just pairwise interactions. Such coupled oscillators provide a Hopfield type networks but with piecewise linear dynamics and hysteretic switching of oscillators. When connected in complex networks with both global and local connectivity, instead of pairwise coupling, these networks of oscillators can be much more powerful and can possibly compute approximate solutions of many hard optimization problems. In one implementation of globally coupled D-R oscillators (with a series resistance), we have recently demonstrated using theory and experimental implementations that such networks are capable of approximating the solution of NP-hard minimum graph coloring problems [35]. When n identical D-R oscillators are coupled using identical capacitors, such network settles to a steady state wherein the relative phases of the oscillators get ordered in a way that corresponds to the solution of graph coloring. The time evolution of the piecewise linear dynamical system of such coupled D-R oscillators inherits the properties of and hence mimics approximate graph coloring algorithms because of the construction of such networks. Basic functioning of such a system is shown in Figure 7.

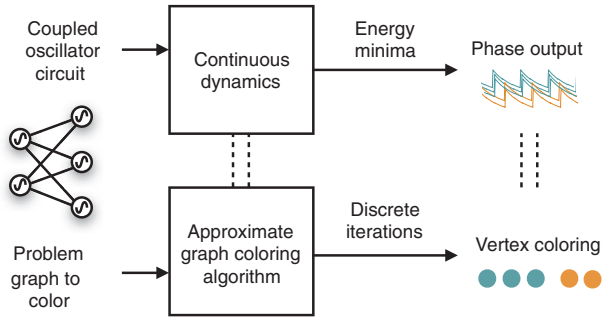

Figure 7: Overview of the proposed graph coloring system using coupled VO_2 oscillators where each node corresponds to a VO_2 oscillator. The dynamics of the system corresponds to an approximate graph coloring algorithm, and as such, the steady-state phase output of the VO_2 oscillators can be used to color the nodes of the graph.

6 Concluding remarks

In this article, we have demonstrated that the dynamics that evolves from the complex interactions among oscillators can be a powerful computing paradigm. However, this requires innovations in fabrication of compact and coupled networks of oscillators, and the current implementation using phase transition devices is one promising candidate. Even with advances in post-silicon devices and technology, the true potential of integrated dynamical systems can only be harnessed when controllable and programmable coupling can be realized and the phase and frequency dynamics carefully measured and read out. A plethora of challenges remain; however, the opportunities offered by dynamical systems to make a significant impact in a post-CMOS world are undeniable.

References

[1] Garey MR, Johnson DS. Computers and intractability: a guide to the theory of NP-completeness. New York, NY, USA: W. H. Freeman & Co, 1979.
[2] Wolfram S, ed. Theory and applications of cellular automata: including selected papers, 1983–1986, no. v. 1 in Advanced series on complex systems. Singapore: World Scientific, 1986.
[3] Shor P. Polynomial-time algorithms for prime factorization and discrete logarithms on a quantum computer. SIAM J Comput 1997;26:1484–509.
[4] Lucas A. Ising formulations of many NP problems. Interdisciplinary Phys 2014;2:5.
[5] Wang Z, Marandi A, Wen K, Byer RL, Yamamoto Y. Coherent Ising machine based on degenerate optical parametric oscillators. Phys Rev A 2013;88:063853.
[6] Hopfield JJ, Tank DW. "Neural" computation of decisions in optimization problems. Biol Cybernetics 1985;52:141–52.
[7] Mostafa H, Müller LK, Indiveri G. An event-based architecture for solving constraint satisfaction problems. Nat Commun 2015;6:8941.
[8] Traversa FL, Ramella C, Bonani F, Di Ventra M. Memcomputing NP-complete problems in polynomial time using polynomial resources and collective states. Sci Adv 2015;1:e1500031.
[9] Chua LO, Yang L. Cellular neural networks: applications. IEEE Trans Circuits Sys 1988;35:1273–90.
[10] Chua LO, Yang L. Cellular neural networks: theory. IEEE Trans Circuits Sys 1988;35:1257–72.
[11] Toffoli T. Cellular automata as an alternative to (rather than an approximation of) differential equations in modeling physics. Phys D Nonlinear Phenom 1984;10:117–27.
[12] Siegelmann HT. Computation beyond the turing limit. Science 1995;268:545–8.
[13] Vergis A, Steiglitz K, Dickinson B. The complexity of analog computation. Math Comput Simul 1986;28:91–113.
[14] Imada M, Fujimori A, Tokura Y. Metal-insulator transitions. Rev Modern Phys 1998;70:1039–263.
[15] Shukla N, Parihar A, Freeman E, et al. Synchronized charge oscillations in correlated electron systems. Sci Rep 2014;4:4964.
[16] Shukla N, Parihar A, Cotter M, et al. Pairwise coupled hybrid vanadium dioxide-MOSFET (HVFET) oscillators for non-boolean associative computing, in Electron Devices Meeting (IEDM), 2014 IEEE International., 28.7.1–28.7.4 (Dec. 2014).
[17] Strogatz SH. From Kuramoto to Crawford: exploring the onset of synchronization in populations of coupled oscillators. Phys D Nonlinear Phenom 2000;143:1–20.
[18] van der Pol B. The nonlinear theory of electric oscillations. in Proceedings of the Institute of Radio Engineers 1934;22:1051–86.
[19] Rand RH, Holmes PJ. Bifurcation of periodic motions in two weakly coupled van der Pol oscillators. Int J Non-Linear Mech 1980;15:387–99.
[20] Storti DW, Rand RH. Dynamics of two strongly coupled van der pol oscillators. Int J Non-Linear Mech 1982;17:143–52.
[21] Kopell N, Somers D. Anti-phase solutions in relaxation oscillators coupled through excitatory interactions. J Math Biol 1995;33:261–80.
[22] Hirano N, Rybicki S. Existence of limit cycles for coupled van der Pol equations. J Differential Equations 2003;195:194–209.
[23] Yogendra K, Fan D, Roy K. Coupled spin torque nano oscillators for low power neural computation. IEEE Trans Magnetics 2015;51:1–9.
[24] Sengupta A, Panda P, Wijesinghe P, Kim Y, Roy K. Magnetic tunnel junction mimics stochastic cortical spiking neurons. Sci Rep 2016;6:30039.
[25] Parihar A, Shukla N, Datta S, Raychowdhury A. Synchronization of pairwise-coupled, identical, relaxation oscillators based on metal-insulator phase transition devices: a model study. J Appl Phys 2015;117:054902.
[26] Datta S, Shukla N, Cotter M, Parihar A, Raychowdhury A. Neuro inspired computing with coupled relaxation oscillators, in Proceedings of The 51st Annual Design Automation Conference on Design Automation Conference, *DAC '14*, 74:1–74:6, ACM, New York, NY, USA, 2014.

[27] Parihar A, Shukla N, Datta S, Raychowdhury A. Exploiting synchronization properties of correlated electron devices in a non-Boolean computing fabric for template matching. IEEE J Emerging Sel Topics Circuits Systems 2014;99:1–10.
[28] Qazilbash MM, Brehm M, Chae BG, et al. Mott transition in VO_2 revealed by infrared spectroscopy and nano-imaging. Science 2007:318:1750–3.
[29] Cavalleri A, Tóth C, Siders CW, et al. Femtosecond structural dynamics in VO_2 during an ultrafast solid-solid phase transition. Phys Rev Lett 2001;87:237401.
[30] Kim BJ, Lee YW, Choi S, et al. Micrometer x-ray diffraction study of VO_2 films: separation between metal-insulator transition and structural phase transition. Phys Rev B 2008;77:235401.
[31] Cao J, Ertekin E, Srinivasan V, et al. Strain engineering and one-dimensional organization of metal-insulator domains in single-crystal vanadium dioxide beams. Nat Nano 2009;4:732–7.
[32] Driscoll T, Kim HT, Chae BG, et al. Memory metamaterials. Science 2009;325:1518–21.
[33] Markov P, Marvel RE, Conley HJ, Miller KJ, Haglund Jr RF, Weiss SM. Optically monitored electrical switching in vo2. ACS Photonics 2015;2:1175–82.
[34] Zhang M, Wiederhecker GS, Manipatruni S, Barnard A, McEuen P, Lipson M. Synchronization of micromechanical oscillators using light. Phys Rev Lett 2012;109:233906.
[35] Parihar A, Shukla N, Jerry M, Datta S, Raychowdhury A. Vertex coloring of graphs via phase dynamics of coupled oscillatory networks. Scientific Reports (in press).